

This is a review of the REVISED MANUSCRIPT performed by Reviewer #3.
All line numbers given below are for the revised version of the manuscript.

The authors have provided additional information that answers most of the comments from the 3 reviewers. However, there are still a few points that need to be addressed before publication in ACP:

We appreciate Reviewer 3's insightful and constructive comments, which significantly improve the manuscript. Please find our response as shown below.

1/ The authors used a catalytic converter to generate zero air from ambient air. The term "VOC-free air" is more appropriate since ambient NO_x are not removed. This zero air is used to perform the "C2" measurement. NO_x will be present in the CRM reactor during both the "C3" measurement, when ambient air is sampled, but also during the "C2" measurement. Since OH can react with NO and NO₂ during both "C3" and "C2", the CRM should be blind to the OH reactivity generated by NO_x. The reported measurements of OH reactivity may therefore be biased low. Interestingly, the authors indicated L185-186 that during the SOAS campaign measurements from the UCI CRM instrument were 16% lower on average than measurements from a LIF system. Could the authors comment on this?

We have discussed the possibility and accept the limitation of this study.
Now it reads:

In conclusion, it is possible that our reported OH reactivity may systematically underestimate ambient total OH reactivity as much as ambient OH reactivity coming from NO₂. (Line 206 - 208, In the track change version)

2/ The authors provided more information about operating conditions for their CRM instrument and indicated that the pyrrole-to-OH ratio was kept constant at a value of 3. This ratio can depend on the amount of OH that is produced from the photolysis of ambient water-vapor in the reactor due to the leakage of 185-nm photons. As a consequence the ratio usually changes with ambient humidity. This ratio was found to vary significantly for other CRM instruments when operated continuously during field campaigns. How did the authors manage to keep the pyrrole-to-OH constant? Was the geometry of the CRM reactor optimized to avoid the photolysis of ambient water-vapor?

We've realized that even with As we are adding 150 cc per minute of humidified N₂ (likely 100 % RH) to the reactor with flow rate of 240 cc per minute, therefore, the variation of ambient humidity change would be dampened quite a bit from the mixing effect. We have included the discussion and now it reads:

Even in the field environment with various relative humidity, we have not observed noticeable changes in this ratio as we flow bulk humidified nitrogen (150 sccm) to the reactor with the total flow of 240 cc, which result in dampening the temporal ambient relative humidity variations. (Line 210 - 213, in the track change version)

Minor comments:

L192-193: “An extensive intercomparison study was conducted by Fuchs et al. (2017) with various OH reactivity measurement techniques that highlighted potential analytical artifacts in the CRM technique. These artifacts have all been examined and preventive measures have been implemented in the UCI CIMS-CRM system deployed at TRF.” - I would add some caveat here since these artefacts have not been fully investigated for this instrument. While some testing has been performed to check whether ambient NO and O₃ could lead to measurement artifacts, the authors acknowledged in their responses to the first review that additional tests are needed to well characterize these artefacts.

We have clarified the limitation in the revised manuscript. Now, it reads:

Again, as the CRM method is relatively new technique, one should keep in mind that the future studies may find potential artifacts that we do not report in this study. (Line 223 - 225, in the track change version)

L200-201: “Our approach to this type of interference has been to determine the maximum NO level, noticeably interfering with the calibration regression line shown in Sanchez et al. (2018). Laboratory tests indicate that the statistical agreement started to veer off when the NO level is 5 ppb in 1 σ of the linear regression” – These tests are of interest for the CRM community and the reviewer recommends to show them in the supplementary material. This will also provide additional confidence in the dataset.

We have added the quantitative information. Now it reads.

Laboratory tests indicate that the statistical agreement started to veer off when the NO level is 5 ppb in 1 σ of the linear regression as the slope for the calibration curve has changed from 0.238 to 0.246. (Line 201 - 203, in the track change version)

L214-216: “In the 2015 field campaigns conducted in Seoul South Korea (Kim et al., 2016), we conducted a standard addition experiment for the propene standard for additional ~ 30 s⁻¹ in two different ozone environment 65 ppb and 123 ppb. The outcome illustrates an agreement between two additions within the analytical uncertainty.” – While a standard addition test could highlight an artefact impacting the linear response of CRM to OH reactivity, it cannot rule out an artefact leading to a positive or negative offset that would only depends on O₃. For the later, a standard addition of 30s⁻¹ of OH reactivity would always lead to the right change in the measured total OH reactivity. However, the total OH reactivity with (ambient reactivity + standard addition reactivity) or without (ambient reactivity) standard addition would be biased low by the same amount. This should be acknowledge in the manuscript.

We have clarified the limitation in the revised manuscript. Now, it reads:

The outcome illustrates an agreement between two additions within the analytical uncertainty although a systematic laboratory study will warrant an accurate uncertainty assessment from ozone. (Line 222 - 224, in the track change version)

L206-211: “Therefore, we performed multi-point calibrations with a propene mixture using a NIST traceable gas standard (AirLiquide LLC, 0.847 ppm) during the field campaign to avoid any circumstances where the pseudo first-order reaction regime is not established.” – Please indicate the range of OH reactivity generated during the multipoint calibration.

We have included the information. Now, it reads:

we performed multi-point calibrations (5 s^{-1} to 30 s^{-1}) with a propene mixture using a NIST traceable gas standard (AirLiquide LLC, 0.847 ppm) during the field campaign to avoid any circumstances where the pseudo first-order reaction regime is not established. (Line 214 - 217, in the track change version)

L244-245: The writing of Eq. 1 is still confusing (mixing of parameters and units). Please only use parameters that are defined in the main text. For instance:

$MR_{\text{voc}} = S_{\text{voc}} \cdot k_{\text{benzene}} / k_{\text{voc}} \cdot 1 / R_{\text{benzene}}$.

MR:Mixing Ratio, S_{voc} : normalized voc signal, k_{benzene} and k_{voc} : proton transfer rate constants, R_{benzene} : benzene sensitivity

We have revised the equation as suggested. Now it reads.

ppb_{voc} is the mixing ratio of an analyte.

$ncps_{\text{voc}}$ is the mass discrimination corrected normalized count for an analyte.

k_{benzene} is the proton transfer reaction rate constant for benzene.

k_{voc} is the proton transfer reaction rate constant for an analyte.

(Line 257 - 260, in the track change version)

**Contributions to OH reactivity from unexplored volatile organic compounds measured by
PTR-ToF-MS– A case study in a suburban forest of the Seoul Metropolitan Area during
KORUS-AQ 2016**

Deleted: -

Dianne Sanchez,¹ Roger Seco,^{1*} Dasa Gu,¹ Alex Guenther,¹ John Mak,² Youngjae Lee,³ Danbi
Kim,³ Joonyoung Ahn,³ Don Blake,⁴ Scott Herndon,⁵ Daun Jeong,¹ John T. Sullivan,⁶ Thomas
Mcgee,⁶ and Saewung Kim^{1*}

1. Department of Earth System Science, University of California, Irvine, Irvine CA 92697,
U.S.A.

2. School of Marine and Atmospheric Sciences, Stony Brooke University, Stony Brook, NY
11794, U.S.A.

3. National Institute of Environmental Research, Inchoen 22689, South Korea

4. Department of Chemistry, University of California, Irvine, Irvine CA 92697, U.S.A.

5. Aerodyne Research Inc., Billerica MA 01821, U.S.A.

6. NASA Goddard Space Flight Center, Chemistry and Dynamics Laboratory, Greenbelt, MD
20771, U.S.A.

* Now at: Terrestrial Ecology Section, Department of Biology, University of Copenhagen,
Copenhagen, Denmark and
Center for Permafrost (CENPERM), Department of Geosciences and Natural Resource
Management, University of Copenhagen, Copenhagen, Denmark

Corresponding author: saewung.kim@uci.edu, tel 1-949-824-4531

To be submitted to Atmospheric Chemistry and Physics

27 **Abstract**

28

29 We report OH reactivity observations by a chemical ionization mass spectrometer –
30 comparative reactivity method (CIMS-CRM) instrument in a suburban forest of the Seoul
31 Metropolitan Area (SMA) during Korea US Air Quality Study (KORUS-AQ 2016) from mid-
32 May to mid-June of 2016. A comprehensive observational suite was deployed to quantify
33 reactive trace gases inside of the forest canopy including a high-resolution proton transfer
34 reaction time of flight mass spectrometer (PTR-ToF-MS). An average OH reactivity of $30.7 \pm$
35 5.1 s^{-1} was observed, while the OH reactivity calculated from CO, NO + NO₂ (NO_x), ozone (O₃),
36 sulfur dioxide (SO₂), and 14 volatile organic compounds (VOCs) was $11.8 \pm 1.0 \text{ s}^{-1}$. An analysis
37 of 346 peaks from the PTR-ToF-MS accounted for an additional $6.0 \pm 2.2 \text{ s}^{-1}$ of the total
38 measured OH reactivity, leaving 42.0 % missing OH reactivity. A series of analyses indicates
39 that the missing OH reactivity most likely comes from VOC oxidation products of both biogenic
40 and anthropogenic origin.

41

42

43

44

45

46

47

48

49

1. Introduction

Total OH reactivity (s^{-1}), the inverse of OH lifetime, is a measure of the total amount of reactive trace gases in the atmosphere in the scale of reactivity, which allow us to quantitatively evaluate our ability to constrain trace gases by comparing measurements of total OH reactivity with the OH reactivity calculated from a speciated reactive gas measurement dataset. The fraction of observed OH reactivity that cannot be reconciled by calculated OH reactivity is known as “missing OH reactivity” (Di Carlo et al., 2004; Goldstein and Galbally, 2007; Yang et al., 2016). A substantial amount of missing OH reactivity has consistently been reported in forest environments (30 - 80%). Di Carlo et al. (2004) conducted a study in a mixed forest near Pellston, Michigan where they reported missing OH reactivity ($\sim 30\%$) larger than observational uncertainty. The authors concluded that the missing sources of reactivity were primary biogenic volatile organic compound (biogenic VOC, BVOC) emissions, as the degree of missing OH reactivity followed the temperature dependence of terpenoid emissions. In a boreal forest in Hyytiälä, Finland, Sinha et al. (2010) report a similar result with observed trace gases that account for only 50% of the measured OH reactivity. They argued that oxidation products of BVOCs alone could not account for the missing OH reactivity. Thus, they also concluded that primary emissions were more likely to be the source of missing OH reactivity and they further suggest that this could be the result of the contribution of small amounts of many reactive gases. Follow up studies (Nolscher et al., 2012; Praplan et al., 2019) at the same site have presented a consistent conclusion. Nolscher et al. (2012) observed the highest level of missing OH reactivity during a heat wave episode, possibly inducing a stress emission response from the local forest. A comprehensive analysis by Praplan et al. (2019) using a long-term observation dataset and a

73 photochemical model framework with the Master Chemical Mechanism illustrates that the model
74 simulated oxidation compound contribution can only contribute 7 % of missing OH reactivity.

75 On the other hand, some studies have attributed the sources of the missing OH reactivity
76 to unmeasured oxidation products of well-characterized BVOCs. Edwards et al. (2013)
77 measured OH reactivity in a pristine tropical forest in the Sabah region of Borneo during the
78 Oxidant and Particle Photochemical Processes (OP3) field campaign (Hewitt et al., 2010). This
79 study implemented the Master Chemical Mechanism (MCMv3.2) (Saunders et al., 2003; Jenkin
80 et al., 1997) into a box model framework to quantify potential contributions from unmeasured
81 oxidation products. The model was constrained with VOCs such as isoprene, monoterpenes, and
82 alkanes and alkenes and other observed trace gases such as $\text{NO} + \text{NO}_2$ (NO_x) and ozone (O_3).
83 The authors reported that the model simulated oxygenated VOCs (OVOCs) could contribute
84 47.1% of the calculated OH reactivity – surpassing the contribution from isoprene, the primary
85 emission of this ecosystem. It is notable that 30% of observed OH reactivity could not be
86 accounted for by the box model simulations. After examining the comprehensive observational
87 suite of VOCs, the authors determined that the most significant missing sources of OH reactivity
88 were likely secondary multifunctional carbon compounds rather than primary BVOC emissions.
89 Hansen et al. (2014) suggested that their observed missing OH reactivity were likely from
90 unmeasured oxidation products during the Community Atmosphere-Biosphere Interaction
91 EXperiment (CABINEX 2009) in Michigan. This notion was also consistent with findings
92 reported by Kim et al. (2011) who measured OH reactivity of branch enclosures from four
93 representative tree species in the forest canopy during the CABINEX study. They reconciled
94 most of the measured OH reactivity of four representative tree species with well-known BVOCs,
95 such as isoprene and monoterpenes. Finally, Nakashima et al. (2014) reported that 29.5% OH

96 reactivity could not be reconciled by the speciated trace gas dataset during the Bio-hydro-
97 atmosphere interactions of Energy, Aerosols, Carbon, H₂O, Organics and Nitrogen-Southern
98 Rocky Mountain 2008 (BEACHON-SMR08) field campaign (Ortega et al., 2014). The campaign
99 took place at the Manitou Experimental Forest (MEF) in Colorado, a ponderosa pine plantation
100 dominated by primary BVOC emissions of 2-methyl-3-butene-2-ol (232-MBO) and
101 monoterpenes (Ortega et al., 2014). The authors also reported that the missing OH reactivity was
102 likely from BVOC oxidation products. In the same context, Kim et al. (2010) conducted PTR-
103 MS mass spectrum analysis for both ambient air and branch enclosures at the MEF site. They
104 reported more conspicuous unidentified signals on PTR-MS mass spectra in the ambient samples
105 than those from branch enclosure samples at this site.

106 During the Southern Oxidant and Aerosol Study (SOAS) in 2013, Kaiser et al. (2016)
107 used a comprehensive suite of VOC measurements at an isoprene dominant forest site in the
108 southeastern US to examine the role of the OVOC species in missing reactive carbon. The
109 authors used MCMv3.2 embedded in the University of Washington Chemical Box Model
110 (UWCM) to compare OH reactivity from model-generated OVOCs to OH reactivity from
111 measurements of OVOCs. There was no significant discrepancy between the average measured
112 and calculated OH reactivity including observed trace gases and model calculated oxidation
113 products of VOCs. However, it was noted that a small portion (1 s^{-1}) of observed OH reactivity
114 could not be reconciled by the model calculation. As this fraction was not correlated to isoprene
115 oxidation products, it was suggested that the missing OH reactivity may be due to unmeasured
116 primary emissions. One caveat of this analysis pointed out by the authors was that the
117 concentrations of the modeled first-generation isoprene oxidation products (e.g. MVK, MACR,
118 isoprene hydroxy hydroperoxides (ISOPOOH), isoprene nitrates (ISOPN), and hydroperoxy

119 aldehydes (HPALD)) were significantly overpredicted in the afternoon. Consequently, the
120 uncertainty of the model calculation is likely to be much higher for the multi-generation
121 oxidation products and their contributions to the OH reactivity contributions. This result
122 highlights the uncertainty in relying solely on box-model results to assess OH reactivity. This
123 *status quo* urges us to take a convergent approach by effectively integrating observational results
124 from novel instrumentation and model outcomes.

125 This study examines the OH reactivity observations at Taehwa Research Forest (TRF)
126 supersite from 15 May 2016 to 7 June 2016 during the Korea United States Air Quality Study
127 2016 (KORUS-AQ 2016) campaign. TRF (37° 18' 19.08" N 127° 19' 7.12" E, 162 m altitude) is
128 operated by Seoul National University and located in Gwangju in the Gyeonggi Province in South
129 Korea (Kim et al., 2013b). The site is about 35 km southeast from the center of Seoul and
130 borders the greater Seoul Metropolitan Area (SMA) with its population of 25.6 million. This
131 geographical proximity to SMA results in a significant level of anthropogenic influence,
132 particularly in elevated NO_x (Kim et al., 2016). Additionally, occasional pollution transport
133 events occur at regional scales. Previous studies at the site have consistently highlighted the
134 importance of BVOC photochemistry at TRF (Kim et al., 2016; Kim et al., 2013a; Kim et al.,
135 2015). Isoprene and monoterpenes are the dominant OH sinks at the site among observed VOCs.
136 The elevated NO_x accelerates the photochemical processing of VOCs (Kim et al., 2015). Thus,
137 this site is an ideal natural laboratory to study contributions towards total OH reactivity from
138 primary trace gas emissions from both natural and anthropogenic processes and their oxidation
139 products. This motivated us to deploy a high-resolution proton transfer reaction time-of-flight
140 mass spectrometer (PTR-ToF-MS) to quantify trace amounts of VOCs with unknown molecular
141 structures by taking advantage of the universal sensitivity of hydronium ion chemistry towards

reactive VOCs (Graus et al., 2010; Jordan et al., 2009a). Therefore, we intend to observationally constrain the contributions of conventionally unidentified or unmeasured VOCs towards OH reactivity.

2. Methods

2.1. Field Site

The Taehwa Research Forest is a Korean pine (*Pinus koraiensis*) plantation (300 m × 300 m) surrounded by a deciduous forest dominated by oak trees (Kim et al., 2013b). A flux tower (40 m height) at the center of TRF has air-sampling inlets at multiple heights (4 m, 8 m, 12 m, and 16 m) below the canopy top (20 m). Each inlet consists of Teflon tubing (3/8" OD) with ~ 1 second of residence time. The trace gas dataset including VOCs presented is the average of concentrations measured at the inlets inside of the canopy as previous studies illustrate that there is no substantial vertical VOC gradients inside of the canopy (within 3 %, Kim et al. (2013b)). An air-conditioned instrument shack located at the base of the flux tower housed the PTR-ToF-MS for VOC measurements, a mini tunable infrared laser direct absorption spectroscopy (mini-TILDAS) instrument for HCHO, methane, and methanol measurements, and analyzers for carbon monoxide (CO), sulfur dioxide (SO₂), ozone (O₃), and meteorological measurements. The OH reactivity and NO_x analyzers were located in another nearby air-conditioned shack (3 m apart) and sampled air through an extended Teflon inlet line of 4 m (1/4" OD) from the ground with a flow rate of 4 sLpm resulting in a 0.5 second residence time. The height of the ambient air intake was 3.5 m. The analytical characteristics of the instrumentation suite are summarized in Table 1. A ceilometer backscattering characterized boundary layer vertical structure at the site. The ceilometer analysis described by Sullivan et al. (2019) reveals the diurnal boundary layer

height evolution, indicating a maximum in the afternoon around 1-3 km and a minimum in the early morning below 500 m.

2.2.OH Reactivity Measurements

A chemical ionization mass spectrometer – comparative reactivity method (CIMS-CRM) instrument was used to measure OH reactivity. The UCI CIMS-CRM system includes a chemical ionization mass spectrometer with a hydronium reagent ion. The CRM method measures total OH reactivity by quantifying the relative loss of pyrrole, a highly reactive gas ($k_{\text{OH}^+ \text{ pyrrole}} = 1.07 \times 10^{-10} \text{ cm}^3 \text{ molecule}^{-1} \text{ s}^{-1}$ at 298 K (Dillon et al., 2012)) that is rarely found in the atmosphere (Sinha et al., 2008b). Nitrogen gas flows through a bubbler full of ultrapure liquid chromatography mass spectrometer (LC-MS) grade water to produce water vapor. The water vapor then flows into a glass reactor where it is photolyzed into OH radicals by a mercury lamp (Pen-Ray® Light Source P/N 90-0012-01). The measurement uncertainty is 16.7% (1σ) with a limit of detection of 4.5 s^{-1} over 2 minutes (3σ).

The UCI CIMS-CRM instrument has been deployed on multiple occasions, including the Megacity Air Pollution Study (MAPS)-Seoul 2015 campaign that incorporated previous measurements at the TRF ground site during September 2015 (Sanchez et al., 2018; Kim et al., 2016). During the SOAS 2013 campaign, an ambient OH reactivity intercomparison study was conducted with laser induced fluorescence (LIF) system (Sanchez et al., 2018). The instrument intercomparison showed that the OH reactivity measurements from the CRM and LIF instruments generally agreed within the analytical uncertainty. An average of 16% difference between the techniques was noted in the late afternoons where the CRM measurements were lower than those from LIF. As discussed in Sanchez et al. (2018), this is likely caused by the

difference in sampling strategies, as the CRM measurements relied on a lengthy Teflon inlet (15 m) while the LIF directly sampled air at the top of a walk up tower. As mentioned above, at TRF we used a shorter inlet line to minimize residence time and avoid inlet line loss.

An extensive intercomparison study was conducted by Fuchs et al. (2017) with various OH reactivity measurement techniques that highlighted potential analytical artifacts in the CRM technique. These artifacts have all been examined and preventive measures have been implemented in the UCI CIMS-CRM system deployed at TRF. This included a laboratory-built catalytic converter (Pt-wool at 350 °C) that minimized the interferences due to changes in air to prevent the interference from the difference in humidity for the zero air characterizations.

Hansen et al. (2015) illustrated that NO_x may be generated from the catalytic converter. To prevent potential NO_x interferences, they used a scrubber with Purafil and activated charcoal, which will modulate the humidity in the sample. Our approach to this type of interference has been to determine the maximum NO level, noticeably interfering with the calibration regression line shown in Sanchez et al. (2018). Laboratory tests indicate that the statistical agreement

started to veer off when the NO level is 5 ppb in 1 σ of the linear regression between instrument response (unitless) and OH reactivity (s^{-1}) as the slope for the calibration curve has changed from 0.238 to 0.246. In addition, Kim et al. (2016) achieved an OH reactivity budget closure in high NO₂ condition, which implies no significant interferences from NO₂. However, in response to the

Fuchs et al. (2017) observation that various CRM configurations suffer from different levels of NO_x interferences, we plan to conduct more systematic NO_x interference tests to more

accurately characterize this system. In conclusion, it is possible that our reported OH reactivity may systematically underestimate ambient total OH reactivity as much as ambient OH reactivity coming from NO₂.

Formatted: Superscript

Formatted: Subscript

211 We consistently kept the pyrrole to OH ratio at 3:1 and so did not ~~achieve a~~ pseudo first
212 order relationship. ~~Even in the field environment with various relative humidity, we have not~~
213 ~~observed noticeable changes in this ratio as we flow bulk humidified nitrogen (150 standard cc~~
214 ~~per minute) to the reactor with the total flow of 240 cc, which result in dampening the temporal~~
215 ~~ambient relative humidity variations.~~ Therefore, we performed multi-point calibrations (~~5 s⁻¹ to~~
216 ~~30 s⁻¹~~) with a propene mixture using a NIST traceable gas standard (AirLiquide LLC, 0.847
217 ppm) during the field campaign to avoid any circumstances where the pseudo first-order reaction
218 regime is not established. Detailed calibration procedures for the OH reactivity system including
219 laboratory multi-component calibration results can be found in Sanchez et al. (2018).

220 In addition, Fuchs et al. (2017) also described a potential interference from ambient O₃ in
221 some CRM systems. In the 2015 field campaigns conducted in Seoul South Korea (Kim et al.,
222 2016), we conducted a standard addition experiment for the propene standard for additional ~ 30
223 s⁻¹ in two different ozone environment 65 ppb and 123 ppb. The outcome illustrates an
224 agreement between two additions within the analytical uncertainty ~~although a systematic~~
225 ~~laboratory study will warrant an accurate uncertainty assessment from ozone. Again, as the CRM~~
226 ~~method is a relatively new technique, one should keep in mind that the future studies may find~~
227 ~~potential artifacts that we do not report in this study.~~

229 **2.3.PTR-ToF-MS Measurements**

230 A high-resolution PTR-TOF-MS (Ionicon Analytik GmbH) (de Gouw and Warneke,
231 2007b) (Jordan et al., 2009b) was deployed at the TRF site. The instrument was operated with a
232 drift tube temperature of 60 °C, 560 V drift voltage, and 2.27 mbar drift tube to maintain E/N of
233 126 Td. Background checks were manually conducted about three times a day for a 10-minute

Deleted: achieve a

Formatted: Superscript

Formatted: Superscript

duration by scrubbing the ambient air through a catalytic convertor (Pt-wool maintained at 350°C). The detectable peaks from the ambient spectra were assessed by subtracting the background spectrum. The instrument was calibrated with a gas mixture manufactured by Apel-Riemer Environmental Inc. The mixture contains ~ 1 ppmv of acetaldehyde, acetone, isoprene, methyl vinyl ketone, methacrolein, benzene, methyl ethyl ketone, toluene, o-xylene, and α -pinene. This standard mixture was only used for the PTR-ToF-MS calibration and not the CRM-CIMS calibration. The concentration of the compounds were assessed in the Blake Lab at University of California, Irvine, who also conducted the airborne VOC analysis using whole air samples during the KORUS-AQ campaign on the NASA DC-8 (Colman et al., 2001).

A mass range of m/z 40 to m/z 267 was analyzed from the recorded PTR-ToF-MS mass spectra. An automatic mass scale calibration was conducted every 5 minutes on the data averaged over 30 seconds. The raw PTR-ToF-MS data were processed using the PTRwid software described by Holzinger (2015). We normalized the mass peaks by 10^6 reagent ion counts (H_3O^+). As the majority of the VOC mass peaks could not be directly calibrated, we determined the VOC sensitivities using equation 1 (Eq 1). This method has been employed by a number of previous studies such as Cappellin et al. (2012). The benzene calibration factor was used to calculate mixing ratios by applying its proton transfer reaction rate coefficient ($k_{benzene}$) and sensitivity ($ncps\ ppb^{-1}$) for the available compounds. The application of this equation can be justified since PTRwid provides the mass discrimination corrected counts as a final computational product.

$$ppb_{VOC} = ncps_{VOC} \times \frac{k_{benzene}}{k_{VOC}} \times \frac{1}{11.94\ ncps\ ppb^{-1}} \quad \text{Eq. 1}$$

where, 11.94 ncps ppb⁻¹ is the assessed sensitivity of benzene.

ppb_{VOC} is the mixing ratio of an analyte.
 $ncps_{VOC}$ is the mass discrimination corrected normalized count for an analyte.
 $k_{benzene}$ is the proton transfer reaction rate constant for benzene.
 k_{VOC} is the proton transfer reaction rate constant for an analyte.

Formatted: Subscript

Formatted: Subscript

Formatted: Font: (Default) Times New Roman

Formatted: Font: (Default) Times New Roman, Subscript

Formatted: Font: (Default) Times New Roman

Formatted: Font: (Default) Times New Roman

Formatted: Font: (Default) Times New Roman

Deleted: ¶

Formatted: Subscript

Formatted: Font: (Asian) Malgun Gothic

For the mass peaks where specific proton transfer reaction rates were unavailable, we estimated the mixing ratios by applying a proton transfer reaction rate coefficient ($k_{H_3O^+}$) of $3.00 \times 10^{-9} \text{ cm}^3 \text{ s}^{-1}$, the default value for PTRwid calculations. The spectra had a limit of detection of tens of ppt for a 30 second average. The calibrated compounds had a range of detection limits as low as 3.7 ppt for α -pinene and as high as 48 ppt for toluene.

2.4. OH Reactivity Calculation

OH reactivity was calculated from the concentrations of all the compounds observed by the instrumental suite described in Table 1. The original data can be found in the KORUS-AQ 2016 data archive at <https://korus-aq.larc.nasa.gov/>. A total of 360 mass peaks measured by the PTR-ToF-MS were analyzed above the background (3σ or above) to assess their contribution to the calculated OH reactivity. Fourteen of the mass peaks were identified as VOCs commonly reported for PTR-MS measurements (Table 1), leaving 346 unidentified peaks. These remaining mass peaks were grouped into three categories in order to estimate their possible OH reactivity contribution.

Category I (81 peaks) included mass peaks for which the PTRwid software calculated a molecular formula. OH reaction rate coefficients for the individual peaks were obtained from the National Institute for Standards and Technology (NIST) Webbook library. As the only

information we have is the molecular composition, we identified multiple isomers with different functional groups and thus different reactivity. We have extensively reviewed previous publications (Williams et al., 2001;De Gouw et al., 2003;de Gouw and Warneke, 2007a;Jordan et al., 2009a;Ruuskanen et al., 2011;Muller et al., 2012;Koss et al., 2017a) identifying ambient VOCs using PTR-MS with both quadrupole and time-of-flight systems to identify possible compounds. For example, for the m/z of 75.043, there are four possible compounds including hydroxy acetone, propionic acid, methyl acetate, and ethyl formate. We used the median reaction constant for the set of possible compounds. The detailed description of the OH reaction constant determination process for the Category I peaks is described in Sanchez (2019). If the information was unavailable from the NIST Webbook database, a structure-reactivity relationship described by Kwok and Atkinson (1995) was applied to obtain reaction rate coefficients. This is an empirical calculation system to estimate k_{OH} based upon the number of carbons and the functional groups of given VOCs. The framework is able to calculate k_{OH} within a factor of two according to a thorough assessments presented in Kwok and Atkinson (1995). However, the authors discourage the application of the framework to compounds that were not examined in the study such as halogenated compounds. Although halogenated compounds are not included in this study, one should be aware of a potentially significant uncertainty.

Category II (28 peaks) included mass peaks for which the PTRwid software could not assess an exact molecular composition due to uncertainty in the data processing system. Nonetheless, this group of compounds illustrated a positive correlation ($R^2 = 0.19$ to 0.88) with either anthropogenic (benzene, toluene) or biogenic (MVK+MACR and monoterpenes) VOCs. Category II compounds are further grouped into subcategories corresponding to these two main VOC sources. OH reaction rate constants (k_{OH}) were estimated with equations based on the

relationship between the m/z and the k_{OH} of compounds in Table 1 (Figure S1). More specifically, we assume that k_{OH} is linearly correlated with m/z . To apply this linear relationship, the compounds with known k_{OH} were grouped into 5 m/z bins and the average k_{OH} of each bin was calculated. The green triangles represent 5 m/z binned averages from these compounds plotted with their respective average k_{OH} . This approach can be justified by the fact that the reaction constants of VOCs towards OH tend to increase as a function of molecular mass within functional groups (Kwok and Atkinson, 1995; Atkinson, 1987). The y-intercepts of the linear regressions were assessed using the k_{OH} values of the biogenic or anthropogenic compounds and their masses.

Category III (237 peaks) included mass peaks with very low mixing ratios (average = 4.8 ppt \pm 19.5 ppt) that were above the limit of detection. We applied a k_{OH} corresponding to the dark green best-fit line in Figure S1 to these peaks. The y-intercept of the dark green line was based on that of acetaldehyde, as it was the lowest mass compound used for the OH reactivity calculations in this study.

There are two components that need to be considered for the assessment of uncertainty associated with calculated OH reactivity: the concentration and the reaction constants with OH. The uncertainty of the observed trace gases is in the range of 5 % to 20 % as shown in Table 1 and is associated with the rate constants from laboratory experiments (Atkinson et al., 2006). Combining 15 % uncertainty from reaction constants and 13.5 % from trace gas observations results in 20 % of uncertainty in calculated OH reactivity. This should be considered as a conservative estimate as most VOC concentrations and associated rate constants are empirically estimated.

3. Results and Discussion

An average OH reactivity of $30.7 \pm 5.1 \text{ s}^{-1}$ was observed from 15 May – 7 June 2016 (Figure 1). This was within the range of OH reactivity observed in urban regions ($10 - 33 \text{ s}^{-1}$) (Kovacs et al., 2003; Ren et al., 2003; Sinha et al., 2008a; Dolgorouky et al., 2012; Whalley et al., 2016; Kim et al., 2016; Yang et al., 2017) and in the range of previously reported observations and model calculations at the TRF site ($\sim 15 - 35 \text{ s}^{-1}$) (Kim et al., 2016; Kim et al., 2015). The total calculated OH reactivity of $11.8 \pm 1.0 \text{ s}^{-1}$ from the measured compounds in Table 1 resulted in 63.3% missing OH reactivity. However, an additional OH reactivity of $6.0 \pm 2.2 \text{ s}^{-1}$ was further calculated from the reactivity of the VOCs in Categories I – III. The contribution lowered the missing OH reactivity level to 42% of the measured OH reactivity. Kim et al. (2016) had previously measured an average OH reactivity of 16.5 s^{-1} at TRF during the MAPS-Seoul campaign from 1 September – 15 September 2015, a substantially lower level than what we report during this springtime study. Although small alkanes and alkenes such as ethane, ethene, propane and propene were not observed on the site, we utilized the dataset from the NASA DC-8 that flew at 700 m above the site, which indicates that their contribution was consistently small ($\sim 0.7 \text{ s}^{-1}$ in average). In this suburban forest, we do not think there is any substantial emission sources of these relatively long-lived VOCs.

The difference can be attributed to the notably higher reactive trace gas loadings during KORUS-AQ compared to the TRF measurements during MAPS-Seoul. The NO_x , benzene, and toluene concentrations were 3 times higher during KORUS-AQ and CO was 1.4 times higher (Figure S2). Although the average isoprene concentrations were similar between the two campaigns, MVK and MACR concentrations during KORUS-AQ were ~ 3 times higher, illustrating a higher oxidative environment. There was a persistently high MVK+MACR to

351 isoprene ratio of 1.8 during the KORUS-AQ campaign at TRF. This ratio was similar to the
352 value reported during the summer in a moderately polluted forest in the Pearl River Delta that
353 was attributed to a strong atmospheric oxidation capacity (Gong et al., 2018). The missing OH
354 reactivity during KORUS-AQ was generally much higher than levels reported during urban
355 observations (up to 50% missing OH reactivity) (Kovacs et al., 2003;Ren et al., 2003;Sinha et
356 al., 2008a;Dolgorouky et al., 2012;Whalley et al., 2016;Kim et al., 2016;Yang et al., 2017) and
357 within the range of previously reported values in forest regions where as much as 80% missing
358 OH reactivity has been reported (Kim et al., 2016;Di Carlo et al., 2004;Nolscher et al.,
359 2012;Edwards et al., 2013;Nolscher et al., 2016;Ramasamy et al., 2018;Nakashima et al., 2014).

360 Figure 2 shows the diurnal average of measured, calculated, and missing OH reactivity
361 from 15 May – 7 June 2016. Isoprene was the largest contributor to VOC OH reactivity in the
362 afternoon and the early evening (36% of the calculated OH reactivity in the evening), consistent
363 with the previous studies conducted in this site (Kim et al., 2016;Kim et al., 2013b;Kim et al.,
364 2015). Among all the trace gases, the largest average contributor to the calculated OH reactivity
365 was NO_x, which contributed 18.2% (5.6 s⁻¹) to the measured OH reactivity. The NO_x
366 contribution to OH reactivity is higher during the morning and evening rush hours and at a
367 minimum in the afternoon, which has been reported consistently in previous reports conducted
368 near megacities (Kovacs et al., 2003;Mao et al., 2010;Dolgorouky et al., 2012;Ren et al.,
369 2003;Shirley et al., 2006). Enhanced OH reactivity during the morning or night and minimum
370 OH reactivity during the afternoon have been reported in urban areas (Kovacs et al., 2003;Ren et
371 al., 2006;Shirley et al., 2006;Dolgorouky et al., 2012;Mao et al., 2010;Whalley et al., 2016). On
372 the other hand, strong light-sensitive biogenic emissions (e.g. isoprene) result in a maximum
373 observed OH reactivity in the afternoon in forested regions (Ren et al., 2006;Sinha et al.,

2012;Edwards et al., 2013;Hansen et al., 2014;Zannoni et al., 2017;Nolscher et al., 2016) . One exception is an OH reactivity observation conducted in Hyytiälä, a forested site that has low isoprene levels, by Sinha et al. (2010). They attributed a flat diurnal OH reactivity variation to the interplay between high daytime emissions and low nighttime boundary layer height. In urban environments, it is mostly anthropogenic trace gases such as aromatics and OVOCs that contribute to OH reactivity. These compounds have a longer lifetime compared to the diurnal boundary layer evolution. This leads to the accumulation of such compounds in the shallow boundary layer during the night. On the other hand, strong emissions of reactive BVOCs in deciduous forest regions enhance OH reactivity during the daytime but then quickly react away. Very subtle diurnal differences observed in this study (Figure 2), therefore, can be understood as the competitive influences of both anthropogenic and biogenic compounds to the OH reactivity.

As described in detail in Sullivan et al. (2019) and Jeong et al. (2019), a strong regional stagnation episode occurred during the KORUS-AQ campaign between May 17 – 23. Later, the Korean Peninsula was affected by a period of continental pollution outflow between May 28 and June 1. The diurnal averages of the two periods and their calculated OH reactivity are presented in Figure 3. It is notable that there is very little difference in the observed OH reactivity between the two distinct periods in terms of the amount of OH reactivity and its diurnal pattern (Figure 4). Furthermore, no significant variance of the different classes of reactive gases such as criteria air pollutants (CO, NO_x, O₃, and SO₂), mostly contributed by NO_x, OVOCs (acetone, acetaldehyde, formaldehyde, methylglyoxal, methanol, methyl ethyl ketone), aromatics (benzene, toluene, xylenes, styrene, benzaldehyde, trimethylbenzenes), and BVOCs (isoprene, monoterpenes, sesquiterpenes, MVK+MACR) was observed during the different periods (Figure 5). These different classes of reactive gases generally differed by less than 10% during the two periods

397 from the overall campaign. This observation shows that the presence of reactive gases is mostly
398 controlled by relatively short-lived compounds determined by local emissions and their oxidation
399 products.

400 The diurnal variation behavior of each chemical class reflects the chemical lifetime of the
401 compounds (e.g. aromatics vs BVOCs). The calculated OH reactivity from OVOCs does not
402 show a strong diurnal variation. This reflects the fact that OVOCs are mostly generated or
403 emitted during the daytime and their lifetime is generally longer than their precursors, which
404 allows nocturnal accumulation due to the absence of OH. The differences in the diurnal variation
405 of different classes of reactive gases can also be used to interpret the origin of the compounds in
406 Categories I-III as presented in Figure 6. The diurnal variations of Category I resemble those of
407 relatively long-lived chemical species with a distinct nocturnal accumulation pattern. This
408 diurnal pattern has been previously reported for both anthropogenic VOCs such as toluene and
409 benzene and temperature dependent monoterpenes such as α -pinene. It is notable that the diurnal
410 pattern is enhanced during the stagnation period during early morning hours. This enhancement
411 is also seen in the aromatic trace gases particularly during the stagnation period (Figure 5b).

412 Indeed, there are both biogenic and anthropogenic contributions towards the Category I
413 compounds, which contribute an average of 3.8 s^{-1} to the OH reactivity assessment, the largest
414 amount among the three categories (Figure 6a). The largest contributors to Category I, which
415 appear to be from a mixture of biogenic and anthropogenic sources, include m/z 89.060, 101.06,
416 and 101.096, and they contributed 0.3 s^{-1} , 0.2 s^{-1} , and 0.2 s^{-1} , respectively. The m/z 89.060 had a
417 molecular formula of $\text{C}_4\text{H}_8\text{O}_2\text{H}^+$ and was correlated to the anthropogenic compounds such as
418 benzene and toluene. The m/z 101.06 peak had the molecular formula of $\text{C}_5\text{H}_8\text{O}_2\text{H}^+$ and had a
419 diurnal variation similar to that of MVK + MACR. This mass peak has been previously

420 identified in laboratory (Zhao et al., 2004) and field (Williams et al., 2001) studies as the C₅
421 hydroxy carbonyl, an isoprene oxidation product. Results from an indoor chamber
422 photooxidation experiment conducted by Lee et al. (2006) showed that *m/z* 101 is a common
423 fragment of unidentified oxidation products of monoterpenes, sesquiterpenes, and isoprene. Lee
424 et al. (2006) also reported that this mass peak also composed over 5% of the fragments of
425 unidentified α - humulene and linalool oxidation products. The molecular formula of this peak is
426 C₆H₁₂OH⁺, and it has been identified in previous studies as C₆ carbonyls (Koss et al., 2017b) or
427 hexanal (Brilli et al., 2014; Rinne et al., 2005). Furthermore, *m/z* 99.044 and 113.023 were also
428 among the highest contributors to Category I and were correlated with MVK and MACR. The
429 *m/z* 99 was previously reported to be a fragment ion of unidentified terpene oxidation products in
430 a chamber experiment (Lee et al., 2006). The *m/z* 113 was observed by a PTR-MS in a
431 Ponderosa pine forest in central California by Holzinger et al. (2005). In this case, it was formed
432 within the canopy from the rapid oxidation of terpinolene, myrcene, and α -terpinene.
433 Furthermore, *m/z* 113 was observed to come from the photooxidation and ozonolysis of multiple
434 terpenes in two indoor chamber studies by Lee et al. (2006). The *m/z* 113 composed over 5% of
435 the oxidation product fragments of myrcene and verbenone. Finally, *m/z* 83.085 had the
436 molecular formula of C₆H₁₁⁺ and was correlated to benzene. Multiple studies have identified this
437 peak as cyclohexane, methyl-cyclopentane, or methylcyclohexane, typically found in areas rich
438 in oil and gas (Koss et al., 2017b; Gueneron et al., 2015; Yuan et al., 2014). In summary, both the
439 gross diurnal pattern and the individual peak analyses consistently illustrates that both
440 anthropogenic and biogenic compounds comprise Category I, the largest contributor to the
441 previously unexplored compounds in the PTR-ToF-MS spectrum at this research site.

442 Category II contributed an average of 0.3 s^{-1} to the calculated OH reactivity, the lowest
443 amount for the three Categories (Figure 6b). The compounds in category II appear to correlate to
444 either BVOCs or acetone, depending on the time period. In Figure 6b, the maximum during the
445 transport period is enhanced to about 0.2 s^{-1} higher than the overall campaign and shifted about 3
446 hours later to ~4:00 PM. The OH reactivity calculated from Category II is strongly correlated to
447 MVK + MACR ($r^2 = 0.82$) during this period as well. On the other hand, during the stagnation
448 period the average OH reactivity from Category II correlates more strongly with acetone ($r^2 =$
449 0.62) than with MVK + MACR ($r^2 = 0.28$). In fact, six of the highest contributors to Category II
450 (Figure 6b) are more strongly correlated to acetone ($r^2 > 0.40$) during the stagnation period
451 compared to the transport period. The sources of acetone can be either biogenic or
452 anthropogenic. Biogenic sources include direct emissions from plants or their oxidation products
453 and plant decay (Jacob et al., 2002; Seco et al., 2007). Anthropogenic sources of acetone include
454 vehicular emissions, solvent use, and the oxidation of other anthropogenic VOCs (Jacob et al.,
455 2002). Therefore, this illustrates that the compounds in Category II also have a complex source
456 profile of both biogenic and anthropogenic origin.

457 Category III contributed 1.9 s^{-1} to the calculated OH reactivity (Figure 6c). The six
458 highest contributors out of 236 mass peaks contributed a total of 0.43 s^{-1} of the calculated OH
459 reactivity. Overall, Category III compounds had no strong correlations to isoprene,
460 MVK+MACR, benzene, or toluene during either the stagnation or transport periods. However,
461 Category III compounds were highly correlated to methylglyoxal ($r^2 = 0.85, 0.82, \text{ and } 0.78$ for
462 the stagnation, transport, and overall period, respectively), one of the measured OVOCs. A
463 global modeling study illustrated that methylglyoxal is mainly produced from isoprene oxidation
464 processes and the second most important source is acetone oxidation (Fu et al., 2008). In

465 addition, aromatics and alkenes are also known to produce methylglyoxal through atmospheric
466 oxidation processes (Henry et al., 2012). As TRF is a high aromatics and high isoprene
467 environment, the source profile of methyl glyoxal in the region is likely complex, which can be
468 applied to interpret the source of the Category III compounds.

469 Overall, the OH reactivity estimates from Categories I – III contributed an average of 6.0
470 $\pm 2.2 \text{ s}^{-1}$ to the calculated OH reactivity. In summary, there is consistency that both
471 anthropogenic and the biogenic contributions need to be further studied in the PTR-ToF-MS
472 spectrum. Furthermore, by adding this additional signal from Category I, II, and III, VOC
473 contribution to calculated OH reactivity (11.0 s^{-1}) becomes larger than that (6.8 s^{-1}) from criteria
474 air pollutants (CO , NO_x , SO_2 and O_3). This should be considered when evaluating ozone
475 production regimes (Kim et al., 2018).

476 Even with the inclusion of the additional peaks to the calculated OH reactivity, we still
477 find a missing OH reactivity of 42%. Thus, it is important to investigate the origin of this
478 missing fraction. A correlation can be observed between missing OH reactivity in percentage and
479 OH reactivity from NO_x ($R^2 = 0.5$, Figure 7 A) but not between OH reactivity from NO_x and
480 absolute missing OH reactivity (s^{-1}) ($R^2 = 0.2$, Figure 7 B). This leads us to speculate that there
481 is a consistent presence of unquantified trace gases, likely oxidation products of both
482 anthropogenic and biogenic VOCs as we explored the origin of the unexplored peaks causing
483 missing OH reactivity. In other words, NO_x is relatively well measured with a highly pronounced
484 temporal variation that determines the percentage of missing OH reactivity.

485 Finally, unaccounted for uncertainty associated with the reaction rate constant
486 estimations described in the method section should be also further explored. For example, to
487 reconcile the averaged missing OH reactivity during the day (10 s^{-1}), it requires $\sim 60 \text{ ppm}$ of

methane but only ~ 4 ppb of isoprene. This clearly demonstrates the importance of rate constant estimation. Indeed, if we apply the reaction rate constant of isoprene with OH ($k_{\text{OH}} = 1 \times 10^{-10} \text{ cm}^3 \text{ molecule}^{-1} \text{ s}^{-1}$ at 298 K) to Category II and Category III compounds, then the observed OH reactivity is fully reconciled (Figure S3). Proton ion chemistry may have an intrinsic limitation to quantify highly oxidized OVOCs. Moreover, due to the different inlet configurations for OH reactivity and VOC observations, their contributions towards observed and calculated OH reactivity may not have been consistently evaluated (e.g. Sanchez et al. (2018)). Therefore, a comprehensive analysis along with a dataset from other instrumentation is necessary towards reconciling missing OH reactivity with observational constraints. Finally, it is highly plausible that we may double count for fragmented molecules in the mass spectrum. Although it would not affect concentration evaluation as the intensity of ion signals from the fragmented molecules would be fully accounted for by adding parent ion and fragmented ion signals, the OH reactivity calculated from the fragmented ions is susceptible to underestimation from the assumption that k_{OH} positively correlates with molecular masses.

502

503 **4. Summary**

504 We present OH reactivity observations at a suburban forest site during the KORUS-AQ field
505 campaign. A comprehensive trace gas dataset including 14 VOCs quantified by PTR-ToF-MS is
506 used to calculate OH reactivity, which only accounts for 36.7 % of the averaged observed OH
507 reactivity.

508 This study presents a detailed methodology for retrieving OH reactivity contributions from
509 all of the peaks of the PTR-ToF-MS mass spectrum. This decreases the amount of missing OH
510 reactivity as the majority of them have not been accounted towards calculated OH reactivity in

previous studies. First, we converted the raw signals to concentrations using a constant proton transfer reaction rate ($3 \times 10^{-9} \text{ cm}^3 \text{ s}^{-1}$). Then, we grouped the previously unaccounted peaks into three categories to estimate reaction constants for each compound. The contributions of the unaccounted peaks in the mass spectrum account for a calculated OH reactivity of $\sim 6 \text{ s}^{-1}$, which decreases missing OH reactivity from 63.3 % to 42.0 %. It is noteworthy that the diurnal variations of observed OH reactivity and calculated OH reactivity from the various groups of trace gases does not have a high variability during the field campaign even though there were several synoptic meteorological configuration changes. This suggests that the reactive trace gas loading is mostly determined by local emission and oxidation processes not influenced by the synoptic meteorological conditions.

In conclusion, this study highlights PTR-ToF-MS as a tool for observationally constraining missing OH reactivity. Further study is required particularly towards characterizing proton reaction rate constants and reaction constants with OH for the many unknown compounds detected on PTR-ToF-MS. In addition, other mass spectrometry techniques, such as nitrate or iodine ion chemistry systems, should be utilized in future studies to complement the PTR technique, which is sensitive to volatile to semi volatile VOCs, to quantify lower volatility compounds and comprehensively constrain OH reactivity contributions from VOCs.

Acknowledgements

This study is supported by NASA (NNX15AT90G) and NIER. We highly appreciate NASA ESPO for logistical support. Taehwa Research Forest is operated by College of Agriculture and Life Sciences at Seoul National University. S. Kim would like to acknowledge a funding support

from Brain Pool Program of National Research Foundation Korea (NRF) Funded by the Ministry of Science ICT (# 2020H1D3A2A01060699).

Data Availability

Data is available at: <https://korus-aq.larc.nasa.gov/>

References

- Atkinson, R.: A Structure-Activity Relationship for the Estimation of Rate Constants for the Gas-Phase Reactions of Oh Radicals with Organic-Compounds, *International Journal of Chemical Kinetics*, 19, 799-828, DOI 10.1002/kin.550190903, 1987.
- Atkinson, R., Baulch, D. L., Cox, R. A., Crowley, J. N., Hampson, R. F., Hynes, R. G., Jenkin, M. E., Rossi, M. J., and Troe, J.: Evaluated kinetic and photochemical data for atmospheric chemistry: Volume II - gas phase reactions of organic species, *Atmospheric Chemistry and Physics*, 6, 3625-4055, 2006.
- Brilli, F., Gioli, B., Ciccioli, P., Zona, D., Loreto, F., Janssens, I. A., and Ceulemans, R.: Proton Transfer Reaction Time-of-Flight Mass Spectrometric (PTR-TOF-MS) determination of volatile organic compounds (VOCs) emitted from a biomass fire developed under stable nocturnal conditions, *Atmospheric Environment*, 97, 54-67, 10.1016/j.atmosenv.2014.08.007, 2014.
- Cappellin, L., Karl, T., Probst, M., Ismailova, K., Winkler, P. M., Soukoulis, C., Aprea, E., Mark, T. D., Gasperi, F., and Biasioli, F.: On quantitative determination of volatile organic compound concentrations using proton transfer reaction Time-of-Flight Mass Spectrometry, *Environment Science & Technology*, 46, 2012.
- Colman, J. J., Swanson, A. L., Meinardi, S., Sive, B. C., Blake, D. R., and Rowland, F. S.: Description of the analysis of a wide range of volatile organic compounds in whole air samples collected during PEM-Tropics A and B, *Analytical Chemistry*, 73, 3723-3731, 2001.
- De Gouw, J., Goldan, P., Warneke, C., Kuster, W., Roberts, J. M., Marchewka, M., Bertman, S. B., Pszenny, A., and Keene, W.: Validation of proton transfer reaction-mass spectrometry (PTR-MS) measurements of gas phase organic compounds in the atmosphere during the New England Air Quality Study (NEAQS) in 2002, *Journal of Geophysical Research*, 108, 4682 doi:4610.1029/2003JD003863, 2003.
- de Gouw, J., and Warneke, C.: Measurements of volatile organic compounds in the earth's atmosphere using proton-transfer-reaction mass spectrometry, *Mass Spectrom Rev*, 26, 223-257, 2007a.

571 de Gouw, J., and Warneke, C.: Measurements of volatile organic compounds in the earth's
 572 atmosphere using proton-transfer-reaction mass spectrometry, *Mass Spectrom Rev*, 26,
 573 223-257, 10.1002/mas.20119, 2007b.
 574 Di Carlo, P., Brune, W. H., Martinez, M., Harder, H., Leshner, R., Ren, X. R., Thornberry, T.,
 575 Carroll, M. A., Young, V., Shepson, P. B., Riemer, D., Apel, E., and Campbell, C.:
 576 Missing OH reactivity in a forest: Evidence for unknown reactive biogenic VOCs,
 577 *Science*, 304, 722-725, Doi 10.1126/Science.1094392, 2004.
 578 Dillon, T. J., Tucceri, M. E., Dulitz, K., Horowitz, A., Vereecken, L., and Crowley, J. N.:
 579 Reaction of Hydroxyl Radicals with C₄H₅N (Pyrrole): Temperature and Pressure
 580 Dependent Rate Coefficients, *Journal of Physical Chemistry A*, 116, 6051-6058,
 581 10.1021/jp211241x, 2012.
 582 Dolgorouky, C., Gros, V., Sarda-Esteve, R., Sinha, V., Williams, J., Marchand, N., Sauvage, S.,
 583 Poulain, L., Sciare, J., and Bonsang, B.: Total OH reactivity measurements in Paris
 584 during the 2010 MEGAPOLI winter campaign, *Atmospheric Chemistry and Physics*, 12,
 585 9593-9612, Doi 10.5194/Acp-12-9593-2012, 2012.
 586 Edwards, P. M., Evans, M. J., Furneaux, K. L., Hopkins, J., Ingham, T., Jones, C., Lee, J. D.,
 587 Lewis, A. C., Moller, S. J., Stone, D., Whalley, L. K., and Heard, D. E.: OH reactivity in
 588 a South East Asian tropical rainforest during the Oxidant and Particle Photochemical
 589 Processes (OP3) project, *Atmospheric Chemistry and Physics*, 13, 9497-9514, Doi
 590 10.5194/Acp-13-9497-2013, 2013.
 591 Fu, T. M., Jacob, D. J., Wittrock, F., Burrows, J. P., Vrekoussis, M., and Henze, D. K.: Global
 592 budgets of atmospheric glyoxal and methylglyoxal, and implications for formation of
 593 secondary organic aerosols, *Journal of Geophysical Research-Atmospheres*, 113, 2008.
 594 Fuchs, H., Novelli, A., Rolletter, M., Hofzumahaus, A., Pfannerstill, E. Y., Kessel, S., Edtbauer,
 595 A., Williams, J., Michoud, V., Dusanter, S., Locoge, N., Zannoni, N., Gros, V., Truong,
 596 F., Sarda-Esteve, R., Cryer, D. R., Brumby, C. A., Whalley, L. K., Stone, D., Seakins, P.
 597 W., Heard, D. E., Schoemaeker, C., Blocquet, M., Coudert, S., Batut, S., Fittschen, C.,
 598 Thames, A. B., Brune, W. H., Ernest, C., Harder, H., Muller, J. B. A., Elste, T., Kubistin,
 599 D., Andres, S., Bohn, B., Hohaus, T., Holland, F., Li, X., Rohrer, F., Kiendler-Scharr, A.,
 600 Tillmann, R., Wegener, R., Yu, Z. J., Zou, Q., and Wahner, A.: Comparison of OH
 601 reactivity measurements in the atmospheric simulation chamber SAPHIR, *Atmospheric*
 602 *Measurement Techniques*, 10, 4023-4053, 2017.
 603 Goldstein, A. H., and Galbally, I. E.: Known and unexplored organic constituents in the earth's
 604 atmosphere, *Environmental Science & Technology*, 41, 1514-1521, 2007.
 605 Gong, D. C., Wang, H., Zhang, S. Y., Wang, Y., Liu, S. C., Guo, H., Shao, M., He, C. R., Chen,
 606 D. H., He, L. Y., Zhou, L., Morawska, L., Zhang, Y. H., and Wang, B. G.: Low-level
 607 summertime isoprene observed at a forested mountaintop site in southern China:
 608 implications for strong regional atmospheric oxidative capacity, *Atmospheric Chemistry*
 609 *and Physics*, 18, 14417-14432, 10.5194/acp-18-14417-2018, 2018.
 610 Graus, M., Muller, M., and Hansel, A.: High Resolution PTR-TOF: Quantification and Formula
 611 Confirmation of VOC in Real Time, *J Am Soc Mass Spectr*, 21, 1037-1044, 2010.
 612 Gueneron, M., Erickson, M. H., VanderSchelden, G. S., and Jobson, B. T.: PTR-MS
 613 fragmentation patterns of gasoline hydrocarbons, *International Journal of Mass*
 614 *Spectrometry*, 379, 97-109, 10.1016/j.ijms.2015.01.001, 2015.
 615 Hansen, R. F., Griffith, S. M., Dusanter, S., Rickly, P. S., Stevens, P. S., Bertman, S. B., Carroll,
 616 M. A., Erickson, M. H., Flynn, J. H., Grossberg, N., Jobson, B. T., Lefer, B. L., and

Wallace, H. W.: Measurements of total hydroxyl radical reactivity during CABINEX 2009-Part 1: field measurements, *Atmospheric Chemistry and Physics*, 14, 2923-2937, 10.5194/acp-14-2923-2014, 2014.

Hansen, R. F., Blocquet, M., Schoemaeker, C., Leonardis, T., Locoge, N., Fittschen, C., Hanoune, B., Stevens, P. S., Sinha, V., and Dusanter, S.: Intercomparison of the comparative reactivity method (CRM) and pump-probe technique for measuring total OH reactivity in an urban environment, *Atmospheric Measurement Techniques*, 8, 4243-4264, 10.5194/amt-8-4243-2015, 2015.

Henry, S. B., Kammrath, A., and Keutsch, F. N.: Quantification of gas-phase glyoxal and methylglyoxal via the Laser-Induced Phosphorescence of (methyl)GLyOxal Spectrometry (LIPGLOS) Method, *Atmospheric Measurement Techniques*, 5, 181-192, 10.5194/amt-5-181-2012, 2012.

Herndon, S. C., Jayne, J. T., Zahniser, M. S., Worsnop, D. R., Knighton, B., Alwine, E., Lamb, B. K., Zavala, M., Nelson, D. D., McManus, J. B., Shorter, J. H., Canagaratna, M. R., Onasch, T. B., and Kolb, C. E.: Characterization of urban pollutant emission fluxes and ambient concentration distributions using a mobile laboratory with rapid response instrumentation, *Faraday Discussions*, 130, 327-339, 10.1039/b500411j, 2005.

Hewitt, C. N., Lee, J. D., MacKenzie, A. R., Barkley, M. P., Carslaw, N., Carver, G. D., Chappell, N. A., Coe, H., Collier, C., Commane, R., Davies, F., Davison, B., Di Carlo, P., Di Marco, C. F., Dorsey, J. R., Edwards, P. M., Evans, M. J., Fowler, D., Furneaux, K. L., Gallagher, M., Guenther, A., Heard, D. E., Helfter, C., Hopkins, J., Ingham, T., Irwin, M., Jones, C., Karunaharan, A., Langford, B., Lewis, A. C., Lim, S. F., MacDonald, S. M., Mahajan, A. S., Malpass, S., McFiggans, G., Mills, G., Misztal, P., Moller, S., Monks, P. S., Nemitz, E., Nicolas-Perea, V., Oetjen, H., Oram, D. E., Palmer, P. I., Phillips, G. J., Pike, R., Plane, J. M. C., Pugh, T., Pyle, J. A., Reeves, C. E., Robinson, N. H., Stewart, D., Stone, D., Whalley, L. K., and Yin, X.: Overview: oxidant and particle photochemical processes above a south-east Asian tropical rainforest (the OP3 project): introduction, rationale, location characteristics and tools, *Atmospheric Chemistry and Physics*, 10, 169-199, 10.5194/acp-10-169-2010, 2010.

Holzinger, R., Lee, A., Paw, K. T., and Goldstein, A. H.: Observations of oxidation products above a forest imply biogenic emissions of very reactive compounds, *Atmospheric Chemistry and Physics*, 5, 67-75, DOI 10.5194/acp-5-67-2005, 2005.

Holzinger, R.: PTRwid: A new widget tool for processing PTR-TOF-MS data, *Atmospheric Measurement Techniques*, 8, 3903-3922, 10.5194/amt-8-3903-2015, 2015.

Jacob, D. J., Field, B. D., Jin, E. M., Bey, I., Li, Q. B., Logan, J. A., Yantosca, R. M., and Singh, H. B.: Atmospheric budget of acetone, *Journal of Geophysical Research-Atmospheres*, 107, Artn 4100, 10.1029/2001jd000694, 2002.

Jenkin, M. E., Saunders, S. M., and Pilling, M. J.: The tropospheric degradation of volatile organic compounds: A protocol for mechanism development, *Atmospheric Environment*, 31, 81-104, Doi 10.1016/S1352-2310(96)00105-7, 1997.

Jeong, D., Seco, R., Gu, D., Lee, Y. R. O., Nault, B. A., Knote, C. J., McGee, T., Sullivan, J. T., Jimenez, J. L., Campuzano-Jost, P., Blake, D. R., Sanchez, D., Guenther, A. B., Tanner, D., Huey, L. G., Long, R., Anderson, B. E., Hall, S. R., Ullmann, K., Shin, H. J., Herndon, S. C., Lee, Y. A. E., Kim, D., Ahn, O. O. Y., and Kim, S.: Integration of airborne and ground observations of nitryl chloride in the Seoul metropolitan area and the

663 implications on regional oxidation capacity during KORUS-AQ 2016, *Atmospheric*
 664 *Chemistry and Physics*, 19, 12779-12795, 10.5194/acp-19-12779-2019, 2019.
 665 Jordan, A., Haidacher, S., Hanel, G., Hartungen, E., Mark, L., Seehauser, H., Schottkowsky, R.,
 666 Sulzer, P., and Mark, T. D.: A high resolution and high sensitivity proton-transfer-
 667 reaction time-of-flight mass spectrometer (PTR-TOF-MS), *International Journal of Mass*
 668 *Spectrometry*, 286, 122-128, 2009a.
 669 Jordan, A., Haidacher, S., Hanel, G., Hartungen, E., Märk, L., Seehauser, H., Schottkowsky, R.,
 670 Sulzer, P., and Märk, T. D.: A high resolution and high sensitivity proton-transfer-
 671 reaction time-of-flight mass spectrometer (PTR-TOF-MS), *Int J Mass Spectrom*, 286,
 672 122-128, <http://dx.doi.org/10.1016/j.ijms.2009.07.005>, 2009b.
 673 Kaiser, J., Skog, K. M., Baumann, K., Bertman, S. B., Brown, S. B., Brune, W. H., Crounse, J.
 674 D., de Gouw, J. A., Edgerton, E. S., Feiner, P. A., Goldstein, A. H., Koss, A., Misztal, P.
 675 K., Nguyen, T. B., Olson, K. F., St Clair, J. M., Teng, A. P., Toma, S., Wennberg, P. O.,
 676 Wild, R. J., Zhang, L., and Keutsch, F. N.: Speciation of OH reactivity above the canopy
 677 of an isoprene-dominated forest, *Atmospheric Chemistry and Physics*, 16, 9349-9359,
 678 10.5194/acp-16-9349-2016, 2016.
 679 Kim, S., Karl, T., Guenther, A., Tyndall, G., Orlando, J., Harley, P., Rasmussen, R., and Apel,
 680 E.: Emissions and ambient distributions of Biogenic Volatile Organic Compounds
 681 (BVOC) in a ponderosa pine ecosystem: interpretation of PTR-MS mass spectra,
 682 *Atmospheric Chemistry and Physics*, 10, 1759-1771, 2010.
 683 Kim, S., Guenther, A., Karl, T., and Greenberg, J.: Contributions of primary and secondary
 684 biogenic VOC to total OH reactivity during the CABINEX (Community Atmosphere-
 685 Biosphere Interactions Experiments)-09 field campaign, *Atmospheric Chemistry and*
 686 *Physics*, 11, 8613-8623, 10.5194/acp-11-8613-2011, 2011.
 687 Kim, S., Wolfe, G. M., Mauldin, L., Cantrell, C., Guenther, A., Karl, T., Turnipseed, A.,
 688 Greenberg, J., Hall, S. R., Ullmann, K., Apel, E., Hornbrook, R., Kajii, Y., Nakashima,
 689 Y., Keutsch, F. N., DiGangi, J. P., Henry, S. B., Kaser, L., Schnitzhofer, R., Graus, M.,
 690 Hansel, A., Zheng, W., and Flocke, F. F.: Evaluation of HOx sources and cycling using
 691 measurement-constrained model calculations in a 2-methyl-3-butene-2-ol (MBO) and
 692 monoterpene (MT) dominated ecosystem, *Atmospheric Chemistry and Physics*, 13, 2031-
 693 2044, Doi 10.5194/Acp-13-2031-2013, 2013a.
 694 Kim, S., Kim, S. Y., Lee, M., Shim, H., Wolfe, G. M., Guenther, A. B., He, A., Hong, Y., and
 695 Han, J.: Impact of isoprene and HONO chemistry on ozone and OVOC formation in a
 696 semirural South Korean forest, *Atmospheric Chemistry and Physics*, 15, 4357-4371, Doi
 697 10.5194/Acp-15-4357-2015, 2015.
 698 Kim, S., Sanchez, D., Wang, M. D., Seco, R., Jeong, D., Hughes, S., Barletta, B., Blake, D. R.,
 699 Jung, J., Kim, D., Lee, G., Lee, M., Ahn, J., Lee, S.-D., Cho, G., Sung, M.-Y., Lee, Y.-
 700 H., Kim, D. B., Kim, Y., Woo, J. H., Jo, D., Park, R., Park, J. H., Hong, Y.-D., and Hong,
 701 J.-H.: OH Reactivity in Urban and Suburban regions in Seoul, South Korea-An East Asia
 702 megacity in a rapid transition, *Faraday Discussions*, DOI:10.1039/C5FD00230C,
 703 DOI:10.1039/C5FD00230C, 2016.
 704 Kim, S., Jeong, D., Sanchez, D., Wang, M., Seco, R., Blake, D., Meinardi, S., Barletta, B.,
 705 Hughes, S., Jung, J., Kim, D., Lee, G., Lee, M., Ahn, J., Lee, S.-D., Cho, G., Sung, M.-
 706 Y., Lee, Y.-H., and Park, R.: The Controlling Factors of Photochemical Ozone
 707 Production in Seoul, South Korea, *Aerosol Air Qual Res*, 18, 2253-2261,
 708 10.4209/aaqr.2017.11.0452, 2018.

709 Kim, S. Y., Jiang, X. Y., Lee, M., Turnipseed, A., Guenther, A., Kim, J. C., Lee, S. J., and Kim,
 710 S.: Impact of biogenic volatile organic compounds on ozone production at the Taehwa
 711 Research Forest near Seoul, South Korea, *Atmospheric Environment*, 70, 447-453, Doi
 712 10.1016/J.Atmosenv.2012.11.005, 2013b.
 713 Koss, A., Yuan, B., Warneke, C., Gilman, J. B., Lerner, B. M., Veres, P. R., Peischl, J.,
 714 Eilerman, S., Wild, R., Brown, S. S., Thompson, C. R., Ryerson, T., Hanisco, T., Wolfe,
 715 G. M., Clair, J. M. S., Thayer, M., Keutsch, F. N., Murphy, S., and de Gouw, J.:
 716 Observations of VOC emissions and photochemical products over US oil- and gas-
 717 producing regions using high-resolution H₃O⁺ CIMS (PTR-ToF-MS), *Atmos. Meas.*
 718 *Tech.*, 10, 2941-2968, 10.5194/amt-10-2941-2017, 2017a.
 719 Koss, A., Yuan, B., Warneke, C., Gilman, J. B., Lerner, B. M., Veres, P. R., Peischl, J.,
 720 Eilerman, S., Wild, R., Brown, S. S., Thompson, C. R., Ryerson, T., Hanisco, T., Wolfe,
 721 G. M., Clair, J. M. S., Thayer, M., Keutsch, F. N., Murphy, S., and de Gouw, J.:
 722 Observations of VOC emissions and photochemical products over US oil- and gas-
 723 producing regions using high-resolution H₃O⁺ CIMS (PTR-ToF-MS), *Atmospheric*
 724 *Measurement Techniques*, 10, 2941-2968, 10.5194/amt-10-2941-2017, 2017b.
 725 Kovacs, T. A., Brune, W. H., Harder, H., Martinez, M., Simpas, J. B., Frost, G. J., Williams, E.,
 726 Jobson, T., Stroud, C., Young, V., Fried, A., and Wert, B.: Direct measurements of urban
 727 OH reactivity during Nashville SOS in summer 1999, *Journal of Environmental*
 728 *Monitoring*, 5, 68-74, 10.1039/b204339d, 2003.
 729 Kwok, E. S. C., and Atkinson, R.: Estimation of Hydroxyl Radical Reaction-Rate Constants for
 730 Gas-Phase Organic-Compounds Using a Structure-Reactivity Relationship - an Update,
 731 *Atmospheric Environment*, 29, 1685-1695, Doi 10.1016/1352-2310(95)00069-B, 1995.
 732 Lee, A., Goldstein, A. H., Kroll, J. H., Ng, N. L., Varutbangkul, V., Flagan, R. C., and Seinfeld,
 733 J. H.: Gas-phase products and secondary aerosol yields from the photooxidation of 16
 734 different terpenes, *Journal of Geophysical Research-Atmospheres*, 111, ArtD17305
 735 10.1029/2006jd007050, 2006.
 736 Mao, J. Q., Ren, X. R., Chen, S. A., Brune, W. H., Chen, Z., Martinez, M., Harder, H., Lefer, B.,
 737 Rappengluck, B., Flynn, J., and Leuchner, M.: Atmospheric oxidation capacity in the
 738 summer of Houston 2006: Comparison with summer measurements in other metropolitan
 739 studies, *Atmospheric Environment*, 44, 4107-4115, 10.1016/j.atmosenv.2009.01.013,
 740 2010.
 741 Muller, M., Graus, M., Wisthaler, A., Hansel, A., Metzger, A., Dommen, J., and Baltensperger,
 742 U.: Analysis of high mass resolution PTR-TOF mass spectra from 1,3,5-trimethylbenzene
 743 (TMB) environmental chamber experiments, *Atmospheric Chemistry and Physics*, 12,
 744 829-843, 10.5194/acp-12-829-2012, 2012.
 745 Nakashima, Y., Kato, S., Greenberg, J., Harley, P., Karl, T., Turnipseed, A., Apel, E., Guenther,
 746 A., Smith, J., and Kajii, Y.: Total OH reactivity measurements in ambient air in a
 747 southern Rocky mountain ponderosa pine forest during BEACHON-SRM08 summer
 748 campaign, *Atmospheric Environment*, 85, 1-8, 2014.
 749 Nolscher, A. C., Williams, J., Sinha, V., Custer, T., Song, W., Johnson, A. M., Axinte, R.,
 750 Bozem, H., Fischer, H., Pouvesle, N., Phillips, G., Crowley, J. N., Rantala, P., Rinne, J.,
 751 Kulmala, M., Gonzales, D., Valverde-Canossa, J., Vogel, A., Hoffmann, T., Ouwersloot,
 752 H. G., de Arellano, J. V. G., and Lelieveld, J.: Summertime total OH reactivity
 753 measurements from boreal forest during HUMPPA-COPEC 2010, *Atmospheric*
 754 *Chemistry and Physics*, 12, 8257-8270, Doi 10.5194/Acp-12-8257-2012, 2012.

755 Nolscher, A. C., Yanez-Serrano, A. M., Wolff, S., de Araujo, A. C., Lavric, J. V., Kesselmeier,
 756 J., and Williams, J.: Unexpected seasonality in quantity and composition of Amazon
 757 rainforest air reactivity, *Nature Communications*, 7, ARTN 10383
 758 10.1038/ncomms10383, 2016.
 759 Ortega, J., Turnipseed, A., Guenther, A. B., Karl, T. G., Day, D. A., Gochis, D., Huffman, J. A.,
 760 Prenni, A. J., Levin, E. J. T., Kreidenweis, S. M., DeMott, P. J., Tobo, Y., Patton, E. G.,
 761 Hodzic, A., Cui, Y. Y., Harley, P. C., Hornbrook, R. S., Apel, E. C., Monson, R. K.,
 762 Eller, A. S. D., Greenberg, J. P., Barth, M. C., Campuzano-Jost, P., Palm, B. B., Jimenez,
 763 J. L., Aiken, A. C., Dubey, M. K., Geron, C., Offenberg, J., Ryan, M. G., Fornwalt, P. J.,
 764 Pryor, S. C., Keutsch, F. N., DiGangi, J. P., Chan, A. W. H., Goldstein, A. H., Wolfe, G.
 765 M., Kim, S., Kaser, L., Schnitzhofer, R., Hansel, A., Cantrell, C. A., Mauldin, R. L., and
 766 Smith, J. N.: Overview of the Manitou Experimental Forest Observatory: site description
 767 and selected science results from 2008 to 2013, *Atmospheric Chemistry and Physics*, 14,
 768 6345-6367, 10.5194/acp-14-6345-2014, 2014.
 769 Praplan, A. P., Tykka, T., Chen, D., Boy, M., Taipale, D., Vakkari, V., Zhou, P. T., Petaja, T.,
 770 and Hellen, H.: Long-term total OH reactivity measurements in a boreal forest,
 771 *Atmospheric Chemistry and Physics*, 19, 14431-14453, 10.5194/acp-19-14431-2019,
 772 2019.
 773 Ramasamy, S., Nagai, Y., Takeuchi, N., Yamasaki, S., Shojia, K., Ida, A., Jones, C., Tsurumaru,
 774 H., Suzuki, Y., Yoshino, A., Shimada, K., Nakashima, Y., Kato, S., Hatakeyama, S.,
 775 Matsuda, K., and Kajii, Y.: Comprehensive measurements of atmospheric OH reactivity
 776 and trace species within a suburban forest near Tokyo during AQUAS-TAMA campaign,
 777 *Atmospheric Environment*, 184, 166-176, 10.1016/j.atmosenv.2018.04.035, 2018.
 778 Ren, X. R., Harder, H., Martinez, M., Leshner, R. L., Oliger, A., Shirley, T., Adams, J., Simpas, J.
 779 B., and Brune, W. H.: HO_x concentrations and OH reactivity observations in New York
 780 City during PMTACS-NY2001, *Atmospheric Environment*, 37, 3627-3637,
 781 10.1016/S1352-2310(03)00460-6, 2003.
 782 Ren, X. R., Brune, W. H., Oliger, A., Metcalf, A. R., Simpas, J. B., Shirley, T., Schwab, J. J.,
 783 Bai, C. H., Roychowdhury, U., Li, Y. Q., Cai, C. X., Demerjian, K. L., He, Y., Zhou, X.
 784 L., Gao, H. L., and Hou, J.: OH, HO₂, and OH reactivity during the PMTACS-NY
 785 Whiteface Mountain 2002 campaign: Observations and model comparison, *Journal of*
 786 *Geophysical Research-Atmospheres*, 111, Artn D10s03
 787 10.1029/2005jd006126, 2006.
 788 Rinne, J., Ruuskanen, T. M., Reissell, A., Taipale, R., Hakola, H., and Kulmala, M.: On-line
 789 PTR-MS measurements of atmospheric concentrations of volatile organic compounds in
 790 a European boreal forest ecosystem, *Boreal Environ Res*, 10, 425-436, 2005.
 791 Ruuskanen, T. M., Mueller, M., Schnitzhofer, R., Karl, T., Graus, M., Bamberger, I., Hortnagl,
 792 L., Brilli, F., Wohlfahrt, G., and Hansel, A.: Eddy covariance VOC emission and
 793 deposition fluxes above grassland using PTR-TOF, *Atmospheric Chemistry and Physics*,
 794 11, 611-625, 2011.
 795 Sanchez, D., Jeong, D., Seco, R., Wrangham, I., Park, J.-H., Brune, W. H., Koss, A., Gilman, J.,
 796 de Gouw, J., Misztal, P., Goldstein, A., Baumann, K., Wennberg, P. O., Keutsch, F. N.,
 797 Guenther, A., and Kim, S.: Intercomparison of OH and OH reactivity measurements in a
 798 high isoprene and low NO environment during the Southern Oxidant and Aerosol Study
 799 (SOAS), *Atmospheric Environment*, 174, 227-236, 10.1016/j.atmosenv.2017.10.056,
 800 2018.

801 Sanchez, D.: Towards the closure of OH reactivity and volatile organic compound budget in the
802 troposphere using in situ observations, Ph. D., Department of Earth System Science,
803 University of California, Irvine, 2019.

804 Saunders, S. M., Jenkin, M. E., Derwent, R. G., and Pilling, M. J.: Protocol for the development
805 of the Master Chemical Mechanism, MCM v3 (Part A): tropospheric degradation of non-
806 aromatic volatile organic compounds, *Atmospheric Chemistry and Physics*, 3, 161-180,
807 2003.

808 Seco, R., Penuelas, J., and Filella, I.: Short-chain oxygenated VOCs: Emission and uptake by
809 plants and atmospheric sources, sinks, and concentrations, *Atmospheric Environment*, 41,
810 2477-2499, 10.1016/j.atmosenv.2006.11.029, 2007.

811 Shirley, T. R., Brune, W. H., Ren, X., Mao, J., Leshner, R., Cardenas, B., Volkamer, R., Molina,
812 L. T., Molina, M. J., Lamb, B., Velasco, E., Jobson, T., and Alexander, M.: Atmospheric
813 oxidation in the Mexico City Metropolitan Area (MCMA) during April 2003,
814 *Atmospheric Chemistry and Physics*, 6, 2753-2765, DOI 10.5194/acp-6-2753-2006,
815 2006.

816 Sinha, V., Williams, J., Crowley, J. N., and Lelieveld, J.: The comparative reactivity method - a
817 new tool to measure total OH reactivity in ambient air, *Atmospheric Chemistry and*
818 *Physics*, 8, 2213-2227, 2008a.

819 Sinha, V., Williams, J., Crowley, J. N., and Lelieveld, J.: The Comparative Reactivity Method
820 ‐ a new tool to measure total OH Reactivity in ambient air, *Atmos. Chem. Phys.*,
821 8, 2213-2227, 10.5194/acp-8-2213-2008, 2008b.

822 Sinha, V., Williams, J., Lelieveld, J., Ruuskanen, T. M., Kajos, M. K., Patokoski, J., Hellen, H.,
823 Hakola, H., Mogensen, D., Boy, M., Rinne, J., and Kulmala, M.: OH Reactivity
824 Measurements within a Boreal Forest: Evidence for Unknown Reactive Emissions,
825 *Environmental Science & Technology*, 44, 6614-6620, Doi 10.1021/Es101780b, 2010.

826 Sinha, V., Williams, J., Diesch, J. M., Drewnick, F., Martinez, M., Harder, H., Regelin, E.,
827 Kubistin, D., Bozem, H., Hosaynali-Beygi, Z., Fischer, H., Andres-Hernandez, M. D.,
828 Kartal, D., Adame, J. A., and Lelieveld, J.: Constraints on instantaneous ozone
829 production rates and regimes during DOMINO derived using in-situ OH reactivity
830 measurements, *Atmospheric Chemistry and Physics*, 12, 7269-7283, Doi 10.5194/Acp-
831 12-7269-2012, 2012.

832 Sullivan, J. T., McGee, T. J., Stauffer, R. M., Thompson, A. M., Weinheimer, A., Knute, C.,
833 Janz, S., Wisthaler, A., Long, R., Szykman, J., Park, J., Lee, Y., Kim, S., Jeong, D.,
834 Sanchez, D., Twigg, L., Sumnicht, G., Knepp, T., and Schroeder, J. R.: Taehwa Research
835 Forest: a receptor site for severe domestic pollution events in Korea during 2016,
836 *Atmospheric Chemistry and Physics*, 19, 5051-5067, 10.5194/acp-19-5051-2019, 2019.

837 Whalley, L. K., Stone, D., Bandy, B., Dunmore, R., Hamilton, J. F., Hopkins, J., Lee, J. D.,
838 Lewis, A. C., and Heard, D. E.: Atmospheric OH reactivity in central London:
839 observations, model predictions and estimates of in situ ozone production, *Atmospheric*
840 *Chemistry and Physics*, 16, 2109-2122, 10.5194/acp-16-2109-2016, 2016.

841 Williams, J., Poschl, U., Crutzen, P. J., Hansel, A., Holzinger, R., Warneke, C., Lindinger, W.,
842 and Lelieveld, J.: An atmospheric chemistry interpretation of mass scans obtained from a
843 proton transfer mass spectrometer flown over the tropical rainforest of Surinam, *Journal*
844 *of Atmospheric Chemistry*, 38, 133-166, Doi 10.1023/A:1006322701523, 2001.

845 Yang, Y. D., Shao, M., Wang, X. M., Nolscher, A. C., Kessel, S., Guenther, A., and Williams, J.:
846 Towards a quantitative understanding of total OH reactivity: A review, *Atmospheric*
847 *Environment*, 134, 147-161, 10.1016/j.atmosenv.2016.03.010, 2016.
848 Yang, Y. D., Shao, M., Kessel, S., Li, Y., Lu, K. D., Lu, S. H., Williams, J., Zhang, Y. H., Zeng,
849 L. M., Noelscher, A. C., Wu, Y. S., Wang, X. M., and Zheng, J. Y.: How the OH
850 reactivity affects the ozone production efficiency: case studies in Beijing and Heshan,
851 China, *Atmospheric Chemistry and Physics*, 17, 7127-7142, 10.5194/acp-17-7127-2017,
852 2017.
853 Yuan, B., Warneke, C., Shao, M., and de Gouw, J. A.: Interpretation of volatile organic
854 compound measurements by proton-transfer-reaction mass spectrometry over the
855 deepwater horizon oil spill, *International Journal of Mass Spectrometry*, 358, 43-48,
856 10.1016/j.ijms.2013.11.006, 2014.
857 Zannoni, N., Gros, V., Esteve, R. S., Kalogridis, C., Michoud, V., Dusanter, S., Sauvage, S.,
858 Locoge, N., Colomb, A., and Bonsang, B.: Summertime OH reactivity from a receptor
859 coastal site in the Mediterranean Basin, *Atmospheric Chemistry and Physics*, 17, 12645-
860 12658, 2017.
861 Zhao, J., Zhang, R. Y., Fortner, E. C., and North, S. W.: Quantification of hydroxycarbonyls
862 from OH-isoprene reactions, *J Am Chem Soc*, 126, 2686-2687, 10.1021/ja0386391,
863 2004.
864

865

866

867

868 Tables and Figures

869

870 Table 1. Description of instrument and measured parameters.

Instrument	Parameters	Measurement Uncertainty (1 σ) and lower level of detection limit
Chemical Ionization Spectroscopy - Comparative Reactivity Method (CIMS-CRM)	OH reactivity	16.7% (5 sec-1)
Thermo Scientific 42i	NO	20% (100 ppt)
Cavity Ring Down Spectroscopy	NO ₂	20% (50 ppt)
Thermo Scientific 49i	O ₃	4% (1 ppb)
Lufft 501 C	Temperature	±0.3 °C (NA)
Thermo Scientific 48i TLE	CO	10% (50 ppb)

Thermo Scientific 43i TLE	SO ₂	10% (100 ppt)
Mini Tunable Infrared Laser Direct Absorption Spectroscopy (mini-TILDAS) Formaldehyde Monitor(Herndon et al., 2005) (Aerodyne Research, Inc)	HCHO, CH ₄ , CH ₃ OH	5% (few tens ppt)
Proton Transfer Reaction Time of Flight Mass Spectrometer (PTR-TOF-MS 8000, IONICON Analytik, GmbH)	Acetaldehyde, Ethanol, Acetone, Isoprene, MVK + MACR, Methyl ethyl ketone, Benzene, Monoterpenes, Toluene, Furfural, Benzaldehyde, Xylenes, Trimethylbenzenes, Sesquiterpenes	Isoprene 9.8% Benzene 6.9% Toluene 6.5% Monoterpenes 9.2% Xylenes 4.0% Other 16.5% (tens ppt)

871

872

873

874

875

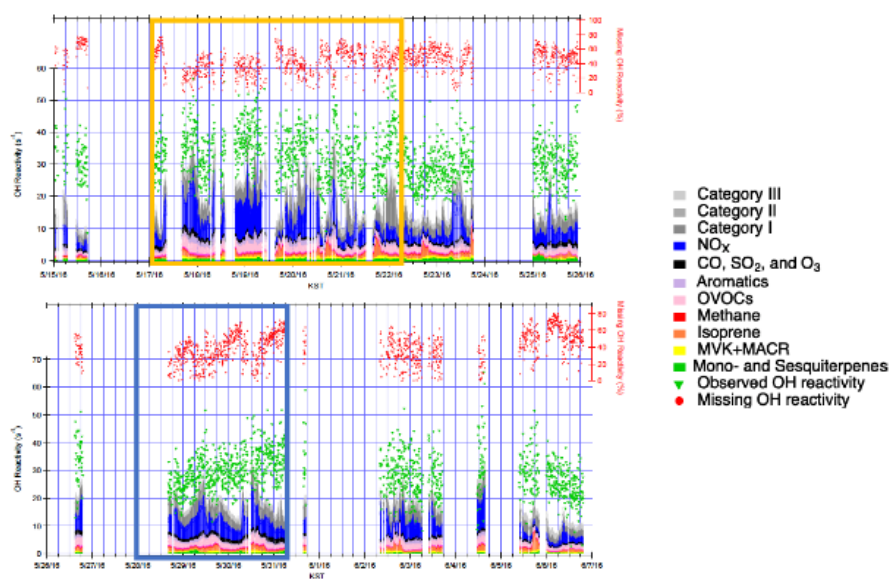
876

877 Figure 1. Observed and calculated OH reactivity during KORUS-AQ 2016. The measured and

878 calculated OH reactivity are on the left axis while the missing OH reactivity is on the right axis.

879 The yellow box represents the stagnation period and the blue box represents the transport period.

880

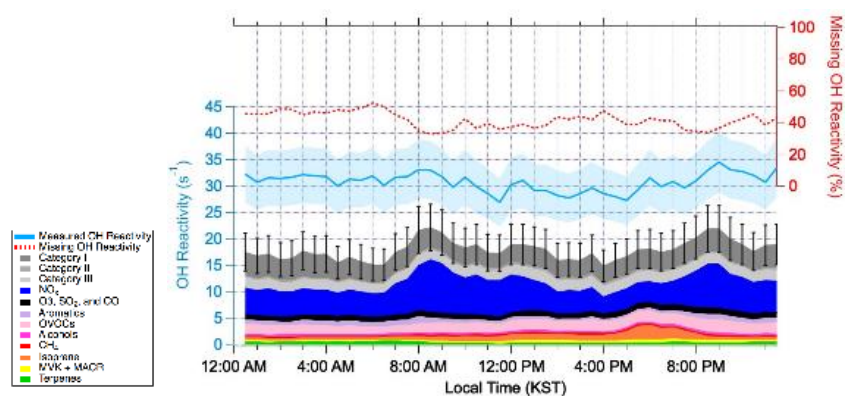


881

882

883 Figure 2. The diurnal average of OH reactivity from 15 May 2016 – 7 June 2016. The measured
 884 and calculated OH reactivity are on the left axis. The blue shading represents uncertainty in the
 885 measured OH reactivity. The black bars represent the propagated uncertainty of calculated OH
 886 reactivity. The missing OH Reactivity in the percentage scale can be read using the right axis.

887



888

889

890

891

892

893

894

895

896

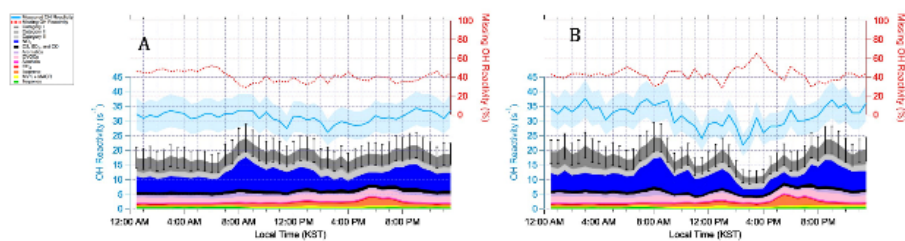
897

898

899

900 Figure 3. Diurnal averages of OH reactivity during the stagnation period (A) from May 17th –
901 May 22nd in 2016 and the transport period (B) from 28 May – 1 June 2016. The measured and
902 calculated OH reactivity are on the left. The blue shading represents an uncertainty of 16.7% at
903 1σ . The black bars represent the propagated uncertainty of 20.1% at 1σ from calculated missing
904 OH reactivity. The percent missing OH reactivity is on the right axis.

905



906

907

908

909

910

911

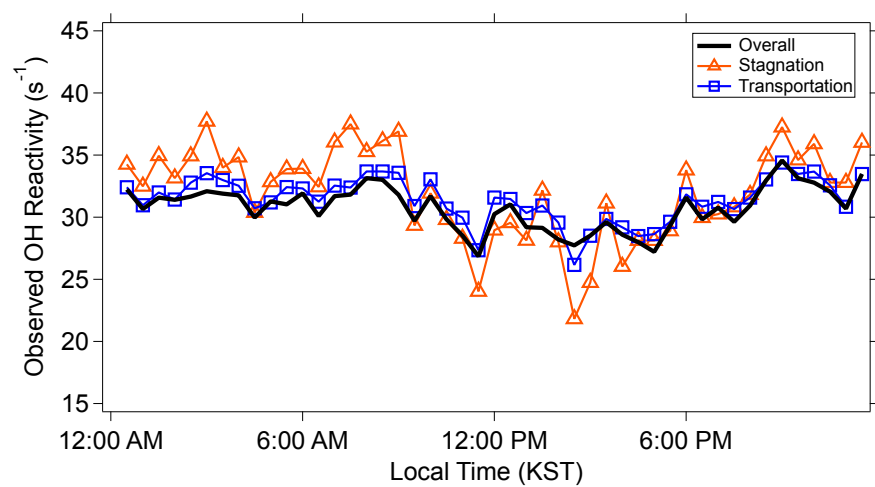
912

913

914

915

916



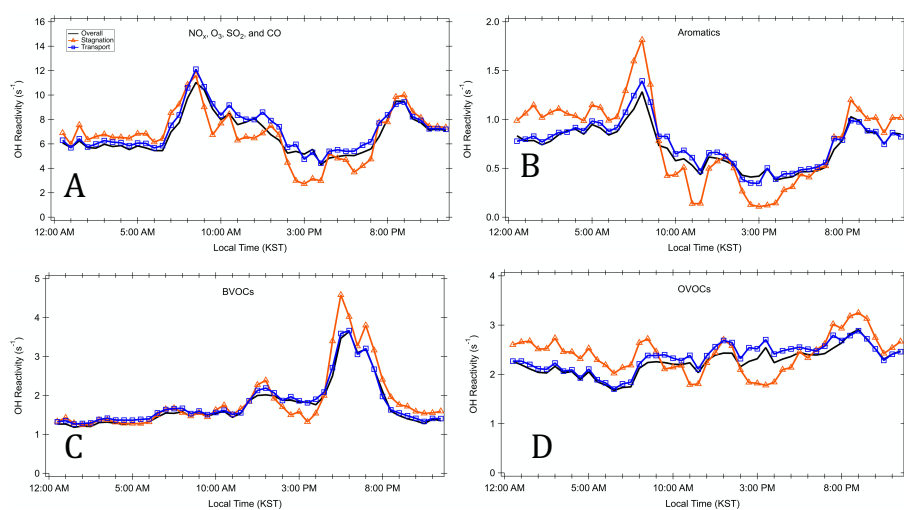
932

933 Figure 5. Diurnal profiles for different classes of trace gases during the different periods. A)

934 criteria pollutants NO_x , O_3 , SO_2 , and CO B) Aromatics, C) BVOCs, and D) OVOCs

935

936



937

938

939

940

941

942

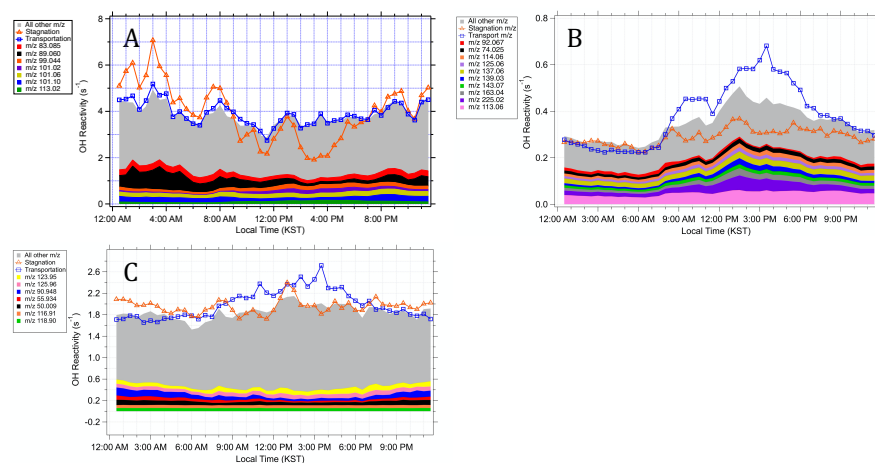
943

944

945

946

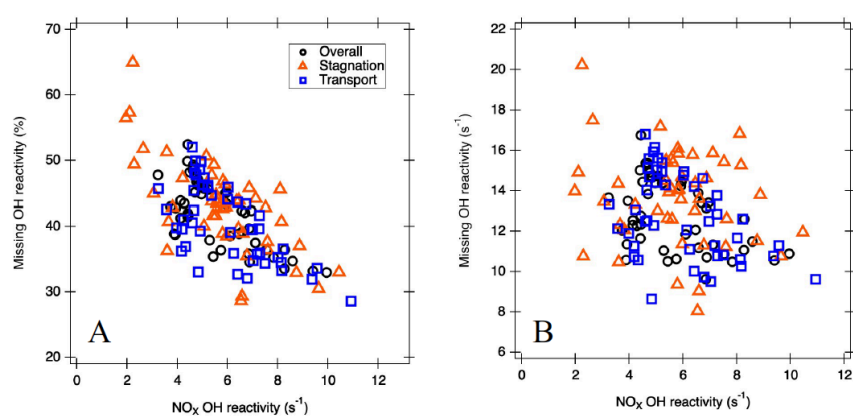
Figure 6. Diurnal averages of the OH reactivity from the compounds in A) Category I, B) Category II and C) Category III



963 Figure 7. The correlation between A) NO_x OH reactivity and absolute missing OH reactivity and
964 B) percent missing OH reactivity

965

966



967